Published in final edited form as:

Prog Brain Res. 2011 ; 194: 131–144. doi:10.1016/B978-0-444-53815-4.00011-X.

Multimodal, longitudinal assessment of intracortical microstimulation

Andrew Koivuniemi[†,§], **Seth J. Wilks**[†], **Andrew J. Woolley**[‡], **Kevin J. Otto**[†,‡,*]

[†]The Weldon School of Biomedical Engineering, Purdue University, West Lafayette, IN, USA

[‡]Department of Biological Sciences, Purdue University, West Lafayette, IN, USA

[§]Indiana University School of Medicine, Indianapolis, IN, USA

Abstract

The fundamental obstacle to neuroprostheses based on penetrating microstimulation is the tissue's response to the device insertion and to the application of the electrical stimulation. Our long-term goal is to develop multichannel microstimulation of central nervous tissue for clinical therapy. The overall objective of this research is to identify the optimal parameters for a chronically implanted microstimulation device. In particular, the work presented here focuses on the effects of repeated stimulation and the reactive tissue response on the efficacy of stimulation-driven behavior. To this end, psychophysical experiments were performed using multichannel cortical implants in the auditory cortex of rats. Further, we investigated the effect of the device–tissue interfacial quality on the psychophysical threshold. Here, we report the effects of cortical depth, days postimplant on the psychophysical threshold of auditory cortical microstimulation, along with correlated impedance spectral changes and *post vivo* histology. We expect that these data will further enable neuroprosthetic development.

Keywords

behavioral; impedance spectroscopy; reactive tissue response; histology; cortical depth

Introduction

Brain machine interfaces (BMIs) aim to transduce information between the world and the subjective experience of the individual. The modern nexus of this dimensional exchange is typically an electrode. From atop the brain or implanted among the glial cells and neurons, the electrode can passively receive or actively drive the dynamics of the local neural cells. This ability to directly interact with the functional networks of the brain has allowed clinicians to lessen the severity of patients' movement disorders (Benabid et al., 2009), grant volitional control over devices to the paralyzed (Hochberg et al., 2006; Kennedy and Bakay, 1998), and create visual sensations in the blind (Schmidt et al., 1996).

*Corresponding author. Tel.: +1-765-496-1012; Fax: +1-765-496-1912, kotto@purdue.edu.

Nonetheless, one serious and nagging problem for many BMIs is failure of effective transduction, putatively due to the reactive tissue response to the indwelling implanted device. Determining whether electrodes can inhabit the brain for decades and continue to interact and provide valuable information is the most significant BMI hurdle. Efforts to develop the proper signal processing techniques and the most effective stimulation patterns are useful endeavors only if the physical connection between the mind and the machine is viable. The answer to the question of long-term device viability varies based on the application. Indeed, for some BMIs, such as deep brain stimulation (Benabid et al., 2009) and surface cortical stimulation (Dobelle, 2000), the issue seems to be mostly resolved, with devices showing functionality extending well beyond 10 years. Further, some arrays used for recording, such as the neurotrophic electrode (Bartels et al., 2008) and cyberkinetics array (Kim et al., 2008), have also showed functionality in humans for years after the initial implantation. However, for systems that rely on the ability of microelectrodes implanted within the cerebral cortex to record and stimulate highly localized cell populations, this problem remains frustratingly unresolved.

This chapter focuses exclusively on intracortical microstimulation (ICMS) of primary sensory cortical structures. After a brief summary of ICMS, it will set forth what is known about the long-term stability of the sensory effects of ICMS in three parts. The first part will discuss the stability of the *behavioral* effect of microstimulation as a function cortical depth. The second will describe the changes in *electrode impedance* seen during electrical stimulation as a potential approach to elucidating changes seen in the behavioral detection level. The final section will describe postmortem *histological* analysis of interfacing tissue as an alternative approach to understanding the behavioral changes.

Background

Stimulation of various sensory cortices offers a versatile platform for sensory prostheses. The logic for this is as follows: (1) Regions of the brain are responsible for processing information from the outside world and, in doing so, generating a perception in the individual. Thus, all awareness of the outside world is a product of this information processing conducted by the networks of neurons. (2) Electric current can be used to artificially drive the activity of those neurons. This driven activity produces an illusory sensation in the subject, the qualities of which are determined by the region that is stimulated. For example, stimulation of the visual cortex creates a visual illusion. Therefore, given points (1) and (2), electrical stimulation of the sensory cortex could restore vision to the blind, hearing to the deaf, and sensation to the paralyzed.

The first well-documented demonstration of electric cortical stimulation's ability to generate sensory illusions was performed by the neurosurgeon Wilder Penfield (Penfield and Boldrey, 1937). Using simple electrodes applied to what is now referred to as the primary somatosensory cortex, Penfield was able to electrically stimulate conscious patients and have them report the evoked sensations, their location, and quality. In doing so, he was able to generate the iconic sensory homunculus. Penfield continued to study the effects of electrical stimulation on the cortex (Penfield and Mullan, 1957; Penfield and Perot, 1963), but his

work tended to focus on higher order structures and was never technologically developed in a way that would lend itself to a sensory prosthesis.

Prosthetic development drove other researchers working in the 1960s and 1970s to systemize the reports of patients receiving cortical stimulation, typically of the primary visual cortex (Brindley and Lewin, 1968; Dobelle and Mladejovsky, 1974). Using surface electrodes placed over the target region, these researchers were able to study the reports of patients and the effects of stimulation parameters either in an acute experiment that only lasted a few minutes during a surgery (Dobelle et al., 1973) or chronically with patients implanted for years (Dobelle, 2000). While the studies did show that some information could be transferred to individuals and that these effects could last years, the large surface electrodes were too limited in terms of the quality and degree of information transferred to make them a viable prosthetic option.

Building on previous work in nonhuman primates (Bartlett and Doty, 1980), another group attempted to improve upon surface stimulation by using microelectrodes implanted within the visual cortex (Bak et al., 1990; Schmidt et al., 1996). These experiments confirmed that ICMS could be employed to increase the density of stimulation electrodes and that they could deliver more channels of information. They also demonstrated that the amount of electric current required to create a detectable sensation in the stimulated individual was two to three orders of magnitude less for ICMS when compared to surface stimulation.

Since that time, work has focused primarily on animal behavioral models. Because the artificially generated sensations require a conscious agent to report on the generated sensation, animals are trained to perform tasks under known physical stimuli which are subsequently replaced by electrical stimuli. Two excellent examples of such tasks can be found in the somatosensory system (O'Doherty et al., 2009; Romo et al., 1998, 2000), where monkeys have been trained to discriminate between the rate of flutter at their finger tips, and in the visual system, where monkeys have learned to perform a delayed saccade to demonstrate where a light appears in their visual field (Murasugi et al., 1993; Salzman et al., 1990; Tehovnik et al., 2003). After the animals perform these tasks in response to known physical stimuli, the behavior is then reelicited using electrical stimuli.

While such elegant tasks are useful in determining the subjective features of ICMS, simple detection tasks in which the animal indicates the presence of a sensation can also be elucidating (Butovas and Schwarz, 2007; Rousche and Normann, 1999). Such studies with simpler tasks are useful for evaluating the stimulation parameters that determine the behavioral salience of the electric pulses because experimenters can rapidly explore a variety of factors (Otto et al., 2005a,b). Additionally, such studies could also be helpful in determining the reliability of ICMS in terms of threshold stability. However, systematic exploration of longitudinal detection thresholds for electrical stimulation is lacking, particularly with regard to the cortical depth of the electrode. Wildly fluctuating or steadily rising thresholds are undesirable and must be avoided if ICMS is to become a clinically viable option for treating individuals with sensory deficits. Here, we report recent data from our laboratory that seeks to assess the *reliability* of ICMS.

Experimental overview

In our behavioral paradigm, water-deprived male Sprague-Dawley rats are trained to perform a conditioned avoidance task to detect a sensory stimulus. This protocol was adapted from earlier studies by Heffner and Kelly (Heffner et al., 1994; Kelly et al., 2006) and is described here only briefly.

After 24 h of water deprivation, a rat is placed in a Coulbourn Instruments (Whitehall, PA) behavioral box in a sound isolated chamber. Water flows through an electrically active drinking spout in response to the rat licking the spout. A pure, unmodulated tone is played for 600 ms and acts as a warning. The rat's licking is monitored for the last 200 ms of the warning. If the rat continues to lick during this period, he receives a mild ~1 mA cutaneous shock delivered through the spout. The amplitude of the next warning stimulus is then raised and a "miss" is recorded. However, if the rat withdraws from the spout during the last 200 ms of the warning trial, a "hit" is recorded and the amplitude of the next stimulus is lowered. After five to seven detection reversals (changes between series of hits and misses), the mean of the final four reversals is calculated and recorded as the detection threshold. This is referred to as the "threshold task," a representative example of which can be seen in Fig. 1c.

To ensure that the rat is maintaining good contact with the spout, warning trials are presented randomly with a 1 in 5 probability, while 4 out of 5 trials are shams in which no warning is presented. If the rat leaves the spout for more than 20% of the sham trials, the series is eliminated from analysis. Once a rat demonstrates that it can consistently perform the task near its putative threshold (Kelly and Masterton, 1977) for a range of frequencies within a single training session, thus generating an audiogram like the one seen in Fig. 1a, it is implanted in its primary auditory cortex (A1) with a single shank, 16 site, 100 μm pitch NeuroNexus (Ann Arbor, MI) microelectrode array in a procedure described in a previous publication (Vetter et al., 2004). During surgery, electrophysiology is performed to ensure that the electrode is placed within the primary auditory cortex and that the site depth is approximately the same for all rats. The electrodes are implanted to span the cortical lamina (Fig. 1b); to confirm cortical depth, local field potentials are recorded, and the current source density is computed to confirm that the electrode array abides in the desired lamina (Müller-Preuss and Mitzdorf, 1984) as seen in Fig. 2.

Behavioral thresholds

Using the adaptive task described above, multiple thresholds can be generated by an animal in a day. Our experimental preparation provides 16 sites linearly over a distance of 1.5 mm, and thus, stimulation can be delivered to all layers of the rat auditory cortex (Paxinos and Watson, 2008), and a behavioral threshold can be generated for all 16 sites in a given rat, each day.

For the experiment presented here, six Sprague-Dawley rats were used (Harlan: Indianapolis, IN) in order to study the effect of electrode site depth on the detection threshold over the first month after implantation. These data, representing 1273 thresholds, have been analyzed in two ways. The first analysis was performed to show the role of depth

on the detection threshold. For the second analysis, the data have been lumped into groups representing four relative cortical depths and displayed by day in order to demonstrate how threshold stability varies over time with cortical depth.

Threshold level varies with depth

Thresholds for all six rats were combined and averaged by electrode site depth. This data is shown in Fig. 3. For the six rats studied, there are three distinct regions in terms of threshold level as follows: The first region is represented by the most superficial sites which are ~0–300 μm below the cortical surface and correspond to the first and second lamina (as schematized in Fig. 1b). These sites have the highest threshold levels and are statistically equivalent. The second region represents a linear transition from the superficial region to the third “deep” region, roughly corresponding to third lamina to fifth lamina. Regression analysis of the threshold means for sites 300–1300 μm deep shows a strong linear correlation (R^2=0.98) with regard to electrode site depth. The third region contains the deepest sites, corresponding to the transition between the fifth and sixth lamina, and has the lowest thresholds. These findings recapitulate previous microstimulation studies performed in the visual cortex which have demonstrated a similar depth-dependent effect (Bak et al., 1990; DeYoe et al., 2005; Tehovnik and Slocum, 2009).

Threshold stability varies with depth

This experiment also helps to elucidate how the depth of the electrode site affects device performance over time. During the 31 days after electrode placement, there appear to be three distinct phases as seen in Fig. 4. In the first phase, which represents the first week after implantation, there is a relatively small difference between the superficial sites and the deep sites. Additionally, there is a gradual rise in the thresholds for all sites. In the second phase, which represents roughly the second week after surgery, the superficial and deep sites begin to separate with threshold levels for the deepest sites declining and the most superficial sites remaining relatively constant. In the third and final phase, thresholds begin to increase again for all but the deepest sites.

Impedance

Implanted electrodes and adjacent tissue form an electrochemical interface that can be characterized via electrochemical measurement techniques. The most common, electrochemical impedance spectroscopy (EIS) measures the impedance magnitude and phase via sinusoidal voltage excitation between the electrode and distant reference at multiple frequencies. EIS provides insight on recording noise levels and safe stimulation levels. Chronic functionality of intracortical microelectrodes requires stable interfacial impedance; however, this is challenging. The reactive tissue response has been shown to affect the impedance at the electrode–tissue interface since encapsulated, damaged tissue display high impedance (Williams et al., 2007). Electrical stimulation can further alter the electrical properties of the tissue, as well as the electrode (Cogan et al., 2004; Weiland and Anderson, 2000; Wilks et al., 2009).

Historical studies show impedance measurements from chronically implanted electrodes showing trends of increasing impedance during the first 2–3 weeks, and then stabilizing, with a reduction in variability between sites and days (Ludwig et al., 2006; Vetter et al., 2004). This trend corresponds well with the time course of the reactive tissue response (Williams et al., 2007). Figure 5a shows average daily 1 kHz impedance magnitude for three probes implanted in three different rats and subjected to daily microstimulation. The impedance increases sharply during the first week after implantation and then gradually decreases back to baseline after day 21. Rather than stabilizing, impedance magnitude and site-to-site variability increase after this point. A similar trend is observed with the day-to-day changes in behavioral thresholds (Fig. 4).

Pronounced changes in the impedance spectra occur after 2 days postimplant and a subsequent trial of microstimulation. As seen in Fig. 5b, the Nyquist plot becomes gradually less linear over the duration of the implant associated with the progression of the reactive tissue response. The original linearity is partially restored after a trial of microstimulation, similar to that seen with *in vivo* voltage biasing (Otto et al., 2006). As previously seen with the *in vivo* biasing, the reduction in impedance is temporary, and the increase in impedance magnitude and variability after 3 weeks of implantation is most likely attributed to tissue and electrode material damage caused by microstimulation amplitudes as high as 50–100 μA (1.6–3.2 mC/cm^2) which exceed the threshold for neural damage (Shannon, 1992) and iridium oxide damage (Cogan et al., 2004; Wilks et al., 2009).

EIS data can be fit to an equivalent circuit model to enable *in vivo* assessment of both the electrode and tissue. As seen in Fig. 6a, the model comprises a constant phase element (CPE) representing the electrode component, a sealing resistance (R_{en}) representing adsorbed proteins, extracellular resistance (R_{ex}), and parallel RC (resistive/capacitive) components representing cell membranes of the glial sheath (Johnson et al., 2005; Otto et al., 2006). The electrode component is broken down into a magnitude (K) and phase scaling term (α), and the membrane component is lumped into a single scaling term (A_m). Figure 6b shows impedance spectra and fitted model data, as well as individual tissue and electrode model components, pre- and postmicrostimulation application. Microstimulation leads to an immediate decrease in impedance with the largest changes occurring in A_m and R_{ex} (Fig. 6c), indicating changes in the encapsulated tissue and extracellular space.

Maintaining a stable, low-impedance interface is important in the continuing functionality of intracortical microelectrodes. Changes in the cellular environment influence the day-to-day impedance changes which are similar to the day-to-day changes in behavioral threshold levels, revealing a complex interaction between the reactive tissue response, changes in electrode properties, and device performance. Repeated microstimulation likely results in additional tissue and electrode damage. However, because the stimulation seems to necessarily disrupt the tissue response adjacent to the electrode site, it is difficult to systematically study this interaction. Nonetheless, it remains an *a priori* truth that the development of devices and techniques to mitigate adverse tissue responses and deliver non-damaging, behaviorally relevant electrical stimulation to the electrode and tissue is essential to maintain a stable, low-impedance interface and a healthy surrounding neural population.

Histology

To investigate whether and how tissue changes at the electrode interface might be affecting long-term device utility, histological labeling and imaging techniques are often employed (Polikov et al., 2005; Stensaas and Stensaas, 1978; Turner et al., 1999). Microscope-based analysis, akin to traditional pathological analysis, can be performed on brain tissue to investigate the tissue response in each subject at a single, final time point. Typically, the locations of applied biomarkers relative to explanted-device holes within each tissue slice are imaged and analyzed. The reason that devices are explanted from tissue is to avoid dragging or shattering them upon slicing the tissue and to simplify the histological preparation. The tissue is thinly sliced in order to both improve the even diffusion of applied biomarker labels and avoid limitations on light penetration through the somewhat opaque tissue upon microscope analysis.

While explanting devices and taking thin (<50 μm) tissue slices has provided significant data on the tissue changes that occur around chronic ICMS arrays (McConnell et al., 2009; Turner et al., 1999; Winslow and Tresco, 2010), this method produces tissue with morphological distortion at the interfacing tissue (Holecko et al., 2005). The former location of electrode sites is also difficult to determine once the device has been explanted. Also, because histological labels diffuse from applied solutions into the tissue, surfaces contacting the solution can have increased labeling, leading to possibly misleading label intensity at the surface of explant holes. To avoid these problems, the authors have developed a method to collect, label, and image the *in situ* implanted device and its surrounding tissue.

Figure 7 presents example microscope data taken around an implanted device, left *in situ* within a thicker (>100 μm) histological slice. Using chemical and immunohistochemical labeling techniques, biomarkers for inflammation, specific cell types, and other items of interest can be fluorescently tagged. After labeling, the tissue and devices can then be imaged using a laser scanning confocal microscope. Images taken along the depth of the intact implant (Fig. 7a and b) allow investigation of tissue changes related to cortical depth. Close investigation of tissue at the device surface or even around individual electrode sites is also performed (Fig. 7c–e), revealing the local distribution of labeled elements relative to the intact electrode–tissue interface.

Conclusion and future work

The development of a functional sensory prosthesis that interfaces directly with the human cortex is a daunting challenge with many obstacles to overcome. However, before any of these may be addressed, it is important to first optimize the electrode design, the implantation technique, and the stimulation parameters.

This chapter reports data and two potential ways of assessing that data. First, the data clearly demonstrate that there is a laminar variation in terms of detection threshold for ICMS in which the deepest sites, roughly corresponding to layers V and VI, are the most sensitive. Second, the data also demonstrate that there is laminar variation in terms of threshold stability over the first month after implantation. Sites that are deepest in cortex maintain

their threshold during the 1-month trial period, while the thresholds for more superficial sites tend to gradually increase. These two facts taken together suggest further investigation of the potential for deep layers to provide consistent stimulation. However, additional work needs to be conducted to determine the source of the laminar variation.

Data addressing the source of the laminar variation may be collected through impedance spectroscopy, which attempts to model the magnitude of the cellular and extracellular tissue response to the implanted electrode. This approach offers an obvious advantage in that it may be performed concurrently with the behavioral task and does not require that the animal be euthanized. A potential hypothesis is that more superficial sites undergo a larger reactive tissue response and, thus, receive the most damage to the neighboring neurons. If this is the case, then those sites should see the greatest increase in impedance levels, signifying that the cellular encapsulation is most virulent at these layers. However, to date, there has not been any strong correlation between electrode impedance values with either site depth or with threshold level. While this may seem to contradict the above hypothesis, it must be noted that the electrical stimulation presents a strong confounding factor by electrical disruption of the glial encapsulation, lowering the impedance as seen in Fig. 6. Future work will focus on refining the model and exploring other parameters that may better correlate with or predict changes in the detection thresholds.

The second potential means of assessing the stability difference between cortical layers is through histology. Using *in situ* techniques which capture the electrode along with the neighboring tissue, we hope to analyze and describe histological markers that could help to explain variations in threshold stability. The primary drawback to this approach is that it requires that the experiment be terminated. Due to the longitudinal behavioral data, animals are often not sacrificed until the device fails or the animal becomes infected. This has frustrated work to fully analyze these effects; therefore, future work will attempt to perform *in vivo* imaging concurrent with the behavioral and impedance spectroscopy measurements.

Finally, additional future work will seek to expand on these findings by exploring novel, potentially more efficient stimulation waveforms, which have been designed to take advantage of the nonlinearities of the voltage-gated sodium channel (McIntyre and Grill, 2000, 2002). Such pulses, employing asymmetric biphasic morphologies, have been shown to lower detection thresholds in cochlear implant users (van Wieringen et al., 2008). However, to the authors' knowledge, these pulses have never been evaluated in the context of ICMS. Additionally, an effort will be made to determine the behavioral safe limits of high duty electrical stimulation using studies similar in design to other chronic stimulation experiments (McCreery et al., 1997, 2002).

References

Bak MJ, Girvin JP, et al. (1990). Visual sensations produced by intracortical microstimulation of the human occipital cortex. Medical & Biological Engineering & Computing, 28(3), 257–259. [PubMed: 2377008]

Bartels J, Andreasen D, et al. (2008). Neurotrophic electrode: Method of assembly and implantation into human motor speech cortex. Journal of Neuroscience Methods, 174(2), 168–176. [PubMed: 18672003]

Bartlett JR, & Doty RW (1980). An exploration of the ability of macaques to detect microstimulation of striate cortex. Acta Neurobiologiae Experimentalis, 40(4), 713–727. [PubMed: 7435271]

Benabid AL, Chabardes S, et al. (2009). Deep brain stimulation of the subthalamic nucleus for the treatment of Parkinson's disease. Lancet Neurology, 8(1), 67–81. [PubMed: 19081516]

Brindley GS, & Lewin WS (1968). The sensations produced by electrical stimulation of the visual cortex. The Journal of Physiology, 196(2), 479–493. [PubMed: 4871047]

Butovas S, & Schwarz C (2007). Detection psychophysics of intracortical microstimulation in rat primary somatosensory cortex. The European Journal of Neuroscience, 25(7), 2161–2169. [PubMed: 17419757]

Cogan SF, Guzelian AA, et al. (2004). Over-pulsing degrades activated iridium oxide films used for intracortical neural stimulation. Journal of Neuroscience Methods, 137(2), 141–150. [PubMed: 15262054]

DeYoe EA, Lewine JD, et al. (2005). Laminar variation in threshold for detection of electrical excitation of striate cortex by macaques. Journal of Neurophysiology, 94(5), 3443–3450. [PubMed: 16079194]

Dobelle WH (2000). Artificial vision for the blind by connecting a television camera to the visual cortex. ASAIO Journal, 46(1), 3–9. [PubMed: 10667705]

Dobelle WH, & Mladejovsky MG (1974). Phosphenes produced by electrical stimulation of human occipital cortex, and their application to the development of a prosthesis for the blind. The Journal of Physiology, 243(2), 553–576. [PubMed: 4449074]

Dobelle WH, Stensaas SS, et al. (1973). A prosthesis for the deaf based on cortical stimulation. The Annals of Otology, Rhinology, and Laryngology, 82(4), 445–463.

Heffner HE, Heffner RS, et al. (1994). Audiogram of the hooded Norway rat. Hearing Research, 73(2), 244–247. [PubMed: 8188553]

Hochberg LR, Serruya MD, et al. (2006). Neuronal ensemble control of prosthetic devices by a human with tetraplegia. Nature, 442(7099), 164–171. [PubMed: 16838014]

Holecko MM 2nd, Williams JC, et al. (2005). Visualization of the intact interface between neural tissue and implanted microelectrode arrays. Journal of Neural Engineering, 2(4), 97–102. [PubMed: 16317233]

Johnson MD, Otto KJ, et al. (2005). Repeated voltage biasing improves unit recordings by reducing resistive tissue impedances. IEEE Transactions on Neural Systems and Rehabilitation Engineering, 13(2), 160–165. [PubMed: 16003894]

Kelly JB, Cooke JE, et al. (2006). Behavioral limits of auditory temporal resolution in the rat: Amplitude modulation and duration discrimination. Journal of Comparative Psychology, 120(2), 98–105. [PubMed: 16719587]

Kelly JB, & Masterton B (1977). Auditory sensitivity of the albino rat. Journal of Comparative and Physiological Psychology, 91(4), 930–936. [PubMed: 893752]

Kennedy PR, & Bakay RAE (1998). Restoration of neural output from a paralyzed patient by a direct brain connection. NeuroReport, 9(8), 1707–1711. [PubMed: 9665587]

Kim S-P, et al. (2008). Neural control of computer cursor velocity by decoding motor cortical spiking activity in humans with tetraplegia. Journal of Neural Engineering, 5(4), 455. [PubMed: 19015583]

Ludwig KA, Uram JD, et al. (2006). Chronic neural recordings using silicon microelectrode arrays electrochemically deposited with a poly(3,4-ethylenedioxythiophene) (PEDOT) film. Journal of Neural Engineering, 3(1), 59–70. [PubMed: 16510943]

McConnell GC, et al. (2009). Implanted neural electrodes cause chronic, local inflammation that is correlated with local neurodegeneration. Journal of Neural Engineering, 6(5), 056003. [PubMed: 19700815]

McCreery DB, Agnew WF, et al. (2002). The effects of prolonged intracortical microstimulation on the excitability of pyramidal tract neurons in the cat. Annals of Biomedical Engineering, 30(1), 107–119. [PubMed: 11874134]

McCreery DB, Yuen TG, et al. (1997). A characterization of the effects on neuronal excitability due to prolonged microstimulation with chronically implanted microelectrodes. IEEE Transactions on Biomedical Engineering, 44(10), 931–939. [PubMed: 9311162]

McIntyre CC, & Grill WM (2000). Selective microstimulation of central nervous system neurons. Annals of Biomedical Engineering, 28(3), 219–233. [PubMed: 10784087]

McIntyre CC, & Grill WM (2002). Extracellular stimulation of central neurons: Influence of stimulus waveform and frequency on neuronal output. Journal of Neurophysiology, 88(4), 1592–1604. [PubMed: 12364490]

Müller-Preuss P, & Mitzdorf U (1984). Functional anatomy of the inferior colliculus and the auditory cortex: Current source density analyses of click-evoked potentials. Hearing Research, 16(2), 133–142. [PubMed: 6526745]

Murasugi CM, Salzman CD, et al. (1993). Microstimulation in visual area MT: Effects of varying pulse amplitude and frequency. The Journal of Neuroscience, 13(4), 1719–1729. [PubMed: 8463847]

O'Doherty JE, Lebedev M, et al. (2009). A brain-machine interface instructed by direct intracortical microstimulation. Frontiers in Neuroengineering, 2(7), 1–8. [PubMed: 19194527]

Otto KJ, Johnson MD, et al. (2006). Voltage pulses change neural interface properties and improve unit recordings with chronically implanted microelectrodes. IEEE Transactions on Biomedical Engineering, 53(2), 333–340. [PubMed: 16485763]

Otto KJ, Rousche PJ, et al. (2005a). Cortical microstimulation in auditory cortex of rat elicits best-frequency dependent behaviors. Journal of Neural Engineering, 2(2), 42–51. [PubMed: 15928411]

Otto KJ, Rousche PJ, et al. (2005b). Microstimulation in auditory cortex provides a substrate for detailed behaviors. Hearing Research, 210(1–2), 112–117. [PubMed: 16209915]

Paxinos G, & Watson C (2007). The rat brain in stereotaxic coordinates. San Diego, CA: Academic Press.

Penfield W, & Boldrey E (1937). Somatic motor and sensory representation in the cerebral cortex of man as studied by electrical stimulation. Brain, 60, 389–443.

Penfield W, & Mullan S (1957). Illusions of perception and the temporal cortex. Transactions of the American Neurological Association 82nd Meeting: 6–8, discussion 8–9.

Penfield W, & Perot P (1963). The brain's record of auditory and visual experience. Brain, 86, 595–696. [PubMed: 14090522]

Polikov VS, Tresco PA, et al. (2005). Response of brain tissue to chronically implanted neural electrodes. Journal of Neuroscience Methods, 148(1), 1–18. [PubMed: 16198003]

Romo R, Hernandez A, et al. (1998). Somatosensory discrimination based on cortical microstimulation. Nature, 392 (6674), 387–390. [PubMed: 9537321]

Romo R, Hernandez A, et al. (2000). Sensing without touching: Psychophysical performance based on cortical microstimulation. Neuron, 26(1), 273–278. [PubMed: 10798410]

Rousche PJ, & Normann RA (1999). Chronic intracortical microstimulation (ICMS) of cat sensory cortex using the Utah Intracortical Electrode Array. IEEE Transactions on Rehabilitation Engineering, 7(1), 56–68. [PubMed: 10188608]

Salzman CD, Britten KH, et al. (1990). Cortical microstimulation influences perceptual judgements of motion direction. Nature, 346(6280), 174–177. [PubMed: 2366872]

Schmidt EM, Bak MJ, et al. (1996). Feasibility of a visual prosthesis for the blind based on intracortical microstimulation of the visual cortex. Brain, 119(Pt. 2), 507–522. [PubMed: 8800945]

Shannon RV (1992). A model of safe levels for electrical stimulation. IEEE Transactions on Biomedical Engineering, 39(4), 424–426. [PubMed: 1592409]

Stensaas SS, & Stensaas LJ (1978). Histopathological evaluation of materials implanted in cerebral-cortex. Acta Neuropathologica, 41(2), 145–155. [PubMed: 636844]

Tehovnik EJ, & Slocum WM (2009). Depth-dependent detection of microampere currents delivered to monkey V1. The European Journal of Neuroscience, 29(7), 1477–1489. [PubMed: 19519630]

Tehovnik EJ, Slocum WM, et al. (2003). Saccadic eye movements evoked by microstimulation of striate cortex. The European Journal of Neuroscience, 17(4), 870–878. [PubMed: 12603277]

Turner JN, Shain W, et al. (1999). Cerebral astrocyte response to micromachined silicon implants. Experimental Neurology, 156(1), 33–49. [PubMed: 10192775]

van Wieringen A, Macherey O, et al. (2008). Alternative pulse shapes in electrical hearing. Hearing Research, 242(1–2), 154–163. [PubMed: 18468821]

Vetter RJ, Williams JC, et al. (2004). Chronic neural recording using silicon-substrate microelectrode arrays implanted in cerebral cortex. IEEE Transactions on Biomedical Engineering, 51(6), 896–904. [PubMed: 15188856]

Weiland JD, & Anderson DJ (2000). Chronic neural stimulation with thin-film, iridium oxide electrodes. IEEE Transactions on Biomedical Engineering, 47(7), 911–918. [PubMed: 10916262]

Wilks SJ, Richardson-Burns SM, et al. (2009). Poly(3,4-ethylenedioxythiophene) as a micro-neural interface material for electrostimulation. Frontiers in Neuroengineering, 3(20), 1–8.

Williams JC, Hippensteel JA, et al. (2007). Complex impedance spectroscopy for monitoring tissue responses to inserted neural implants. Journal of Neural Engineering, 4, 410–423. [PubMed: 18057508]

Winslow BD, & Tresco PA (2010). Quantitative analysis of the tissue response to chronically implanted microwire electrodes in rat cortex. Biomaterials, 31(7), 1558–1567. [PubMed: 19963267]

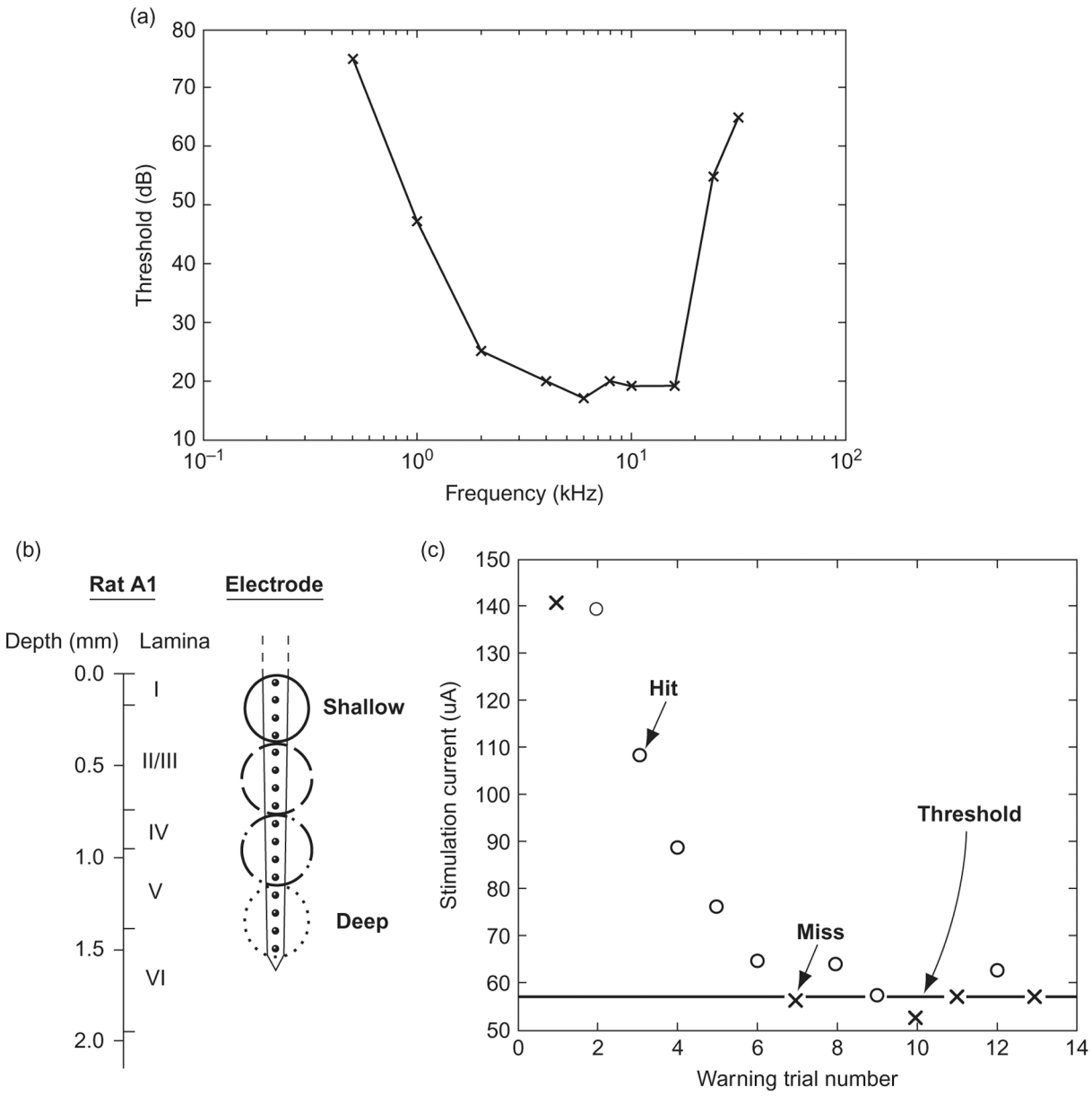

Fig. 1.

Experimental background. (a) Sample audiogram generated by a rat in a single day. (b) Schematic representation of rat auditory cortex delineating histological layers as well as relative electrode site placement. (c) Sample rat adaptive threshold task: "○" represents a hit, "×" represents a miss, the bold line represents the threshold estimate.

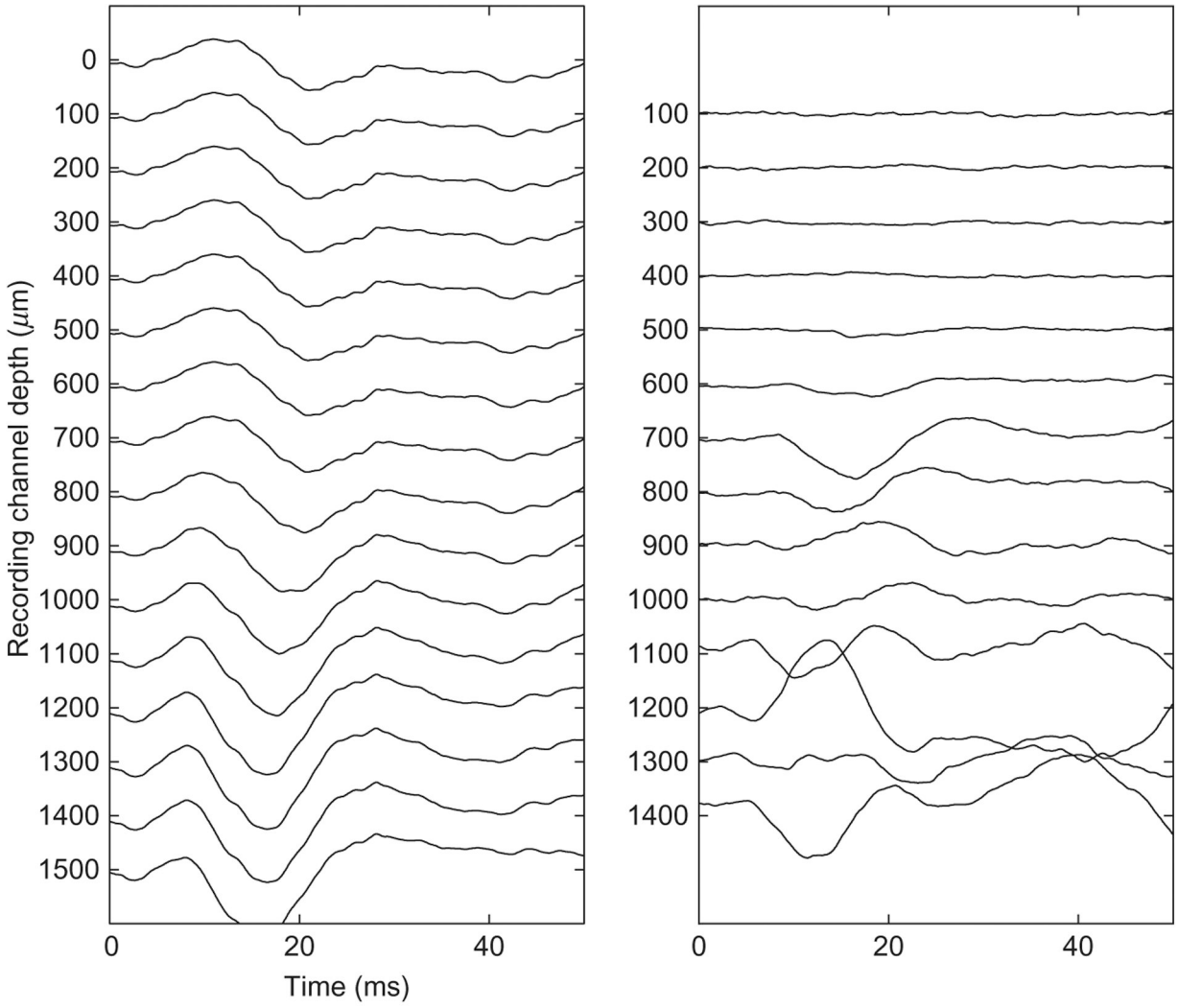

Fig. 2.

Sample recording to determine electrode depth location. The left panel shows the averaged local field potentials. The right panel shows the second spatial derivative of the left panel, a method known as current source density analysis (CSD).

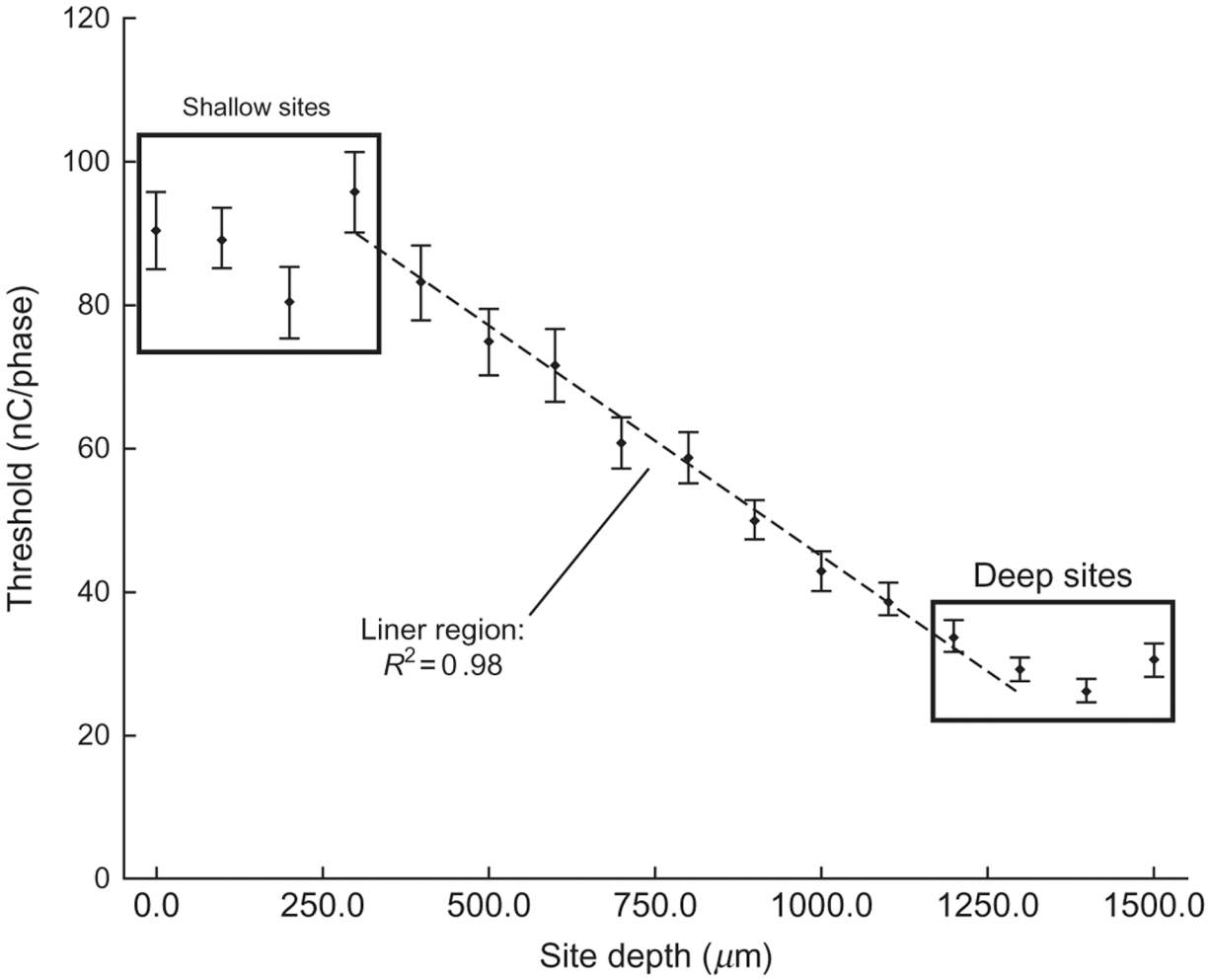

Fig. 3.

Mean thresholds for all six rats averaged by electrode site. Points highlighted as “deep” and “shallow” sites have statistically equivalent threshold levels. The linear region represents a transition zone. Regression analysis was performed on the threshold mean from 300 to 1300 μm deep. Error bars show the standard error of the mean.

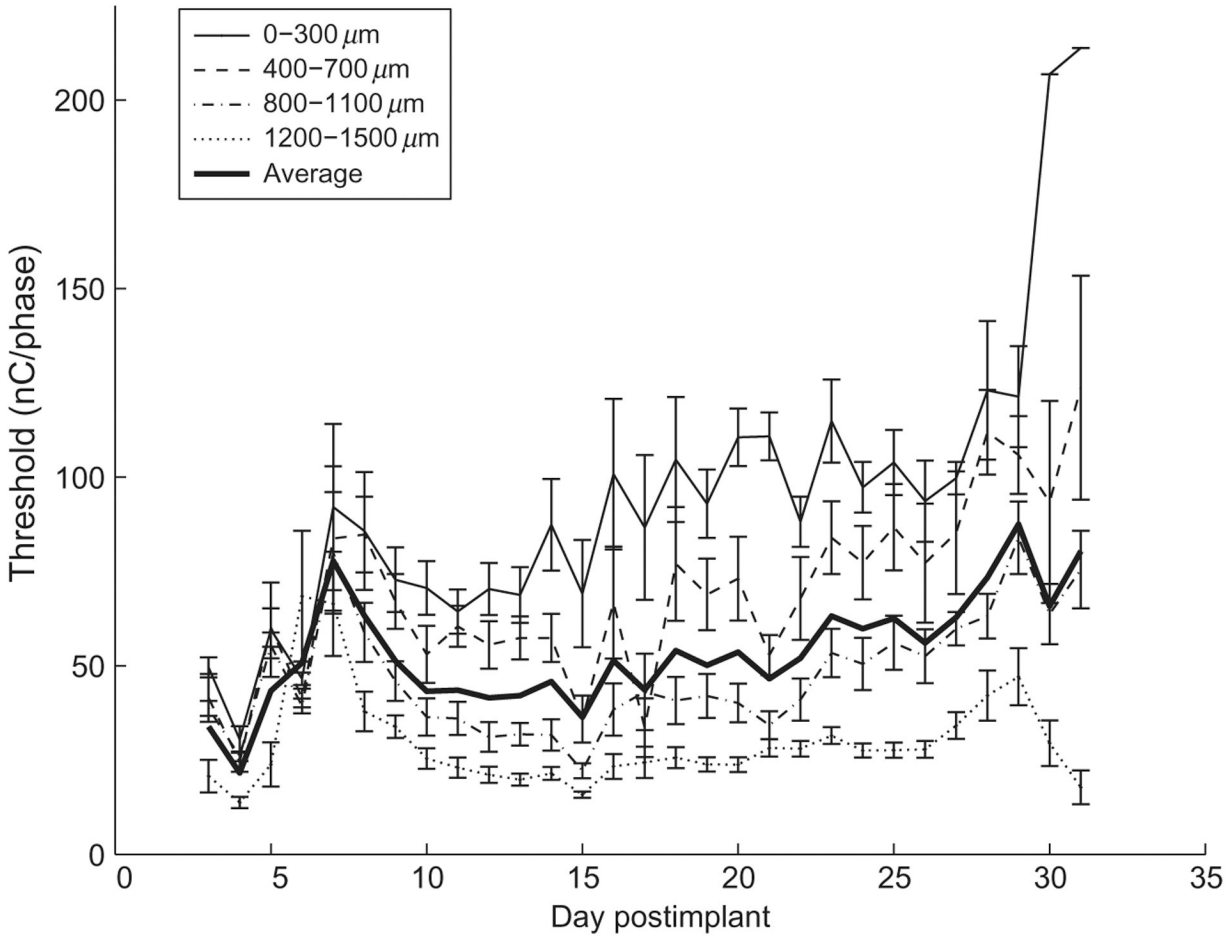

Fig. 4.

Mean thresholds (represented on the *Y*-axis) for all six rats lumped into depth regions and averaged by days postimplant. The threshold, that is, the current amplitude for which the rat's detection probability equaled 50%, is represented in terms of nC per phase, which is the product of the current amplitude and the duration of the first phase. The data represent the first month (31 days) after implantation. In the first week (days 1–7), thresholds tend to rise together. In the second week (days 8–14), thresholds tend to recover with deeper sites decreasing the most. In the final phase, thresholds tend to increase in the superficial sites, while thresholds at deep sites are relatively stable. Error bars show the standard error of the mean.

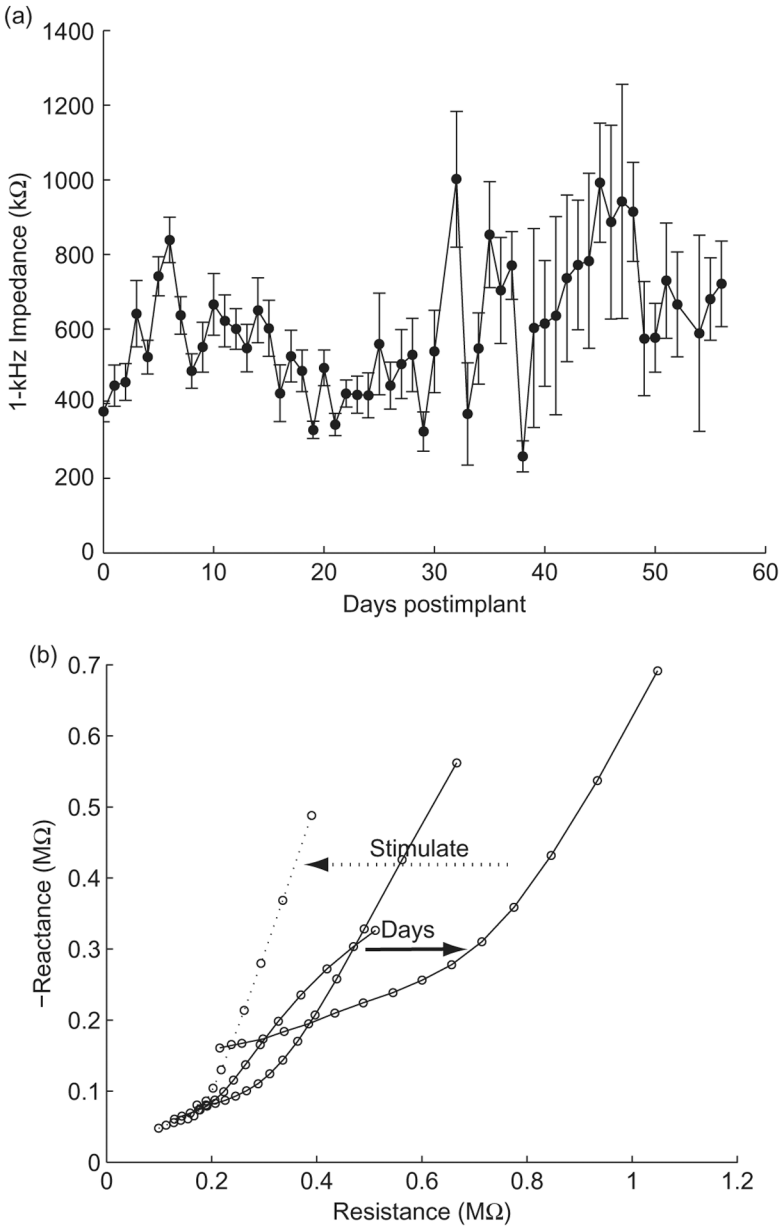

Fig. 5.

Impedance stability over time. (a) Mean 1 kHz impedance magnitudes from three electrodes arrays implanted in three different rats subjected to daily microstimulation. Consistent across each implantation, the impedance magnitude increases with time postimplant. (b) Nyquist plots from three electrode arrays taken immediately after implantation, 1 and 2 days postimplant (solid lines), and immediately after electrical stimulation (dotted line). This is an example of typical trends in impedance changes after implantation and electrical stimulation.

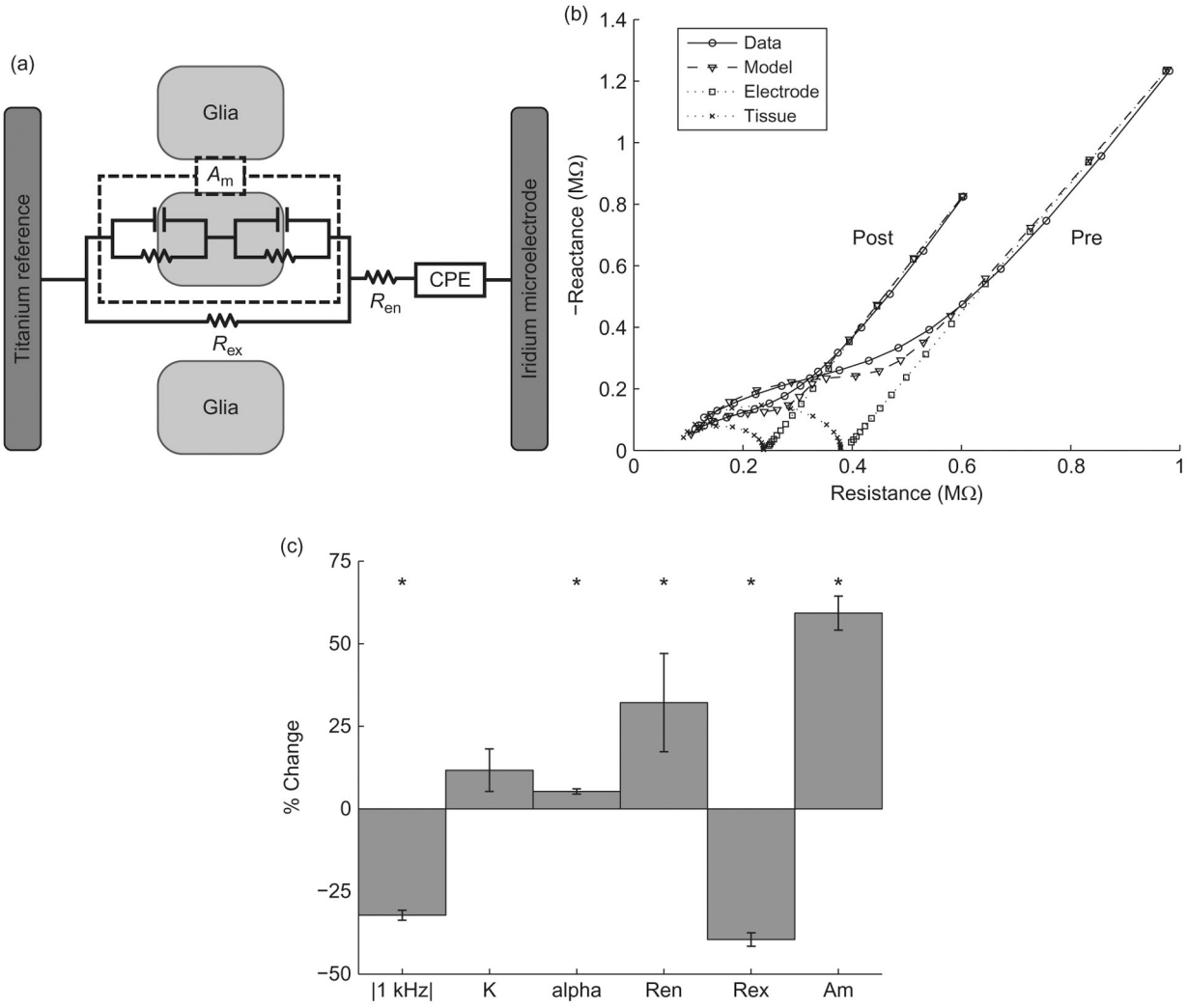

Fig. 6.

Modeling effects of stimulation on electrode impedance. (a) Equivalent circuit model of the electrode–tissue interface.(b) Nyquist plots of measured and modeled impedance spectra from an electrode pre- and postmicrostimulation. (c) Significant changes in 1 kHz impedance and model parameters occur pre- and postmicrostimulation, especially for the tissue components R_{en}, R_{ex}, and A_m (n=350, paired t-test, p<0.01).

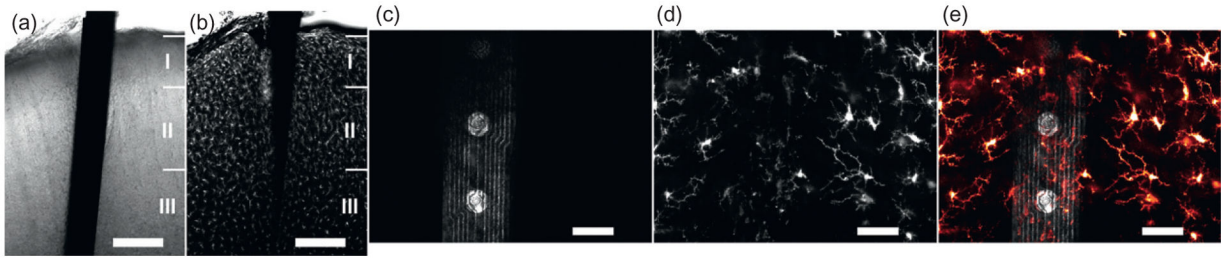

Fig. 7.

In situ histology to investigate the intact device/tissue interface. (a) Transmission light image showing a microelectrode array captured in fixed brain tissue and imaged by laser confocal microscopy. (b) Microglia, labeled by immunohistochemically tagging the protein Iba1 with the fluorescent marker Alexa Fluor 633, are seen in a single optical section responding in a layer-dependent fashion around this 1-week implanted device. (c) A 10-μm-thick *z*-stack of images shows the device surface imaged by collecting laser reflectance; (d) microglia at this same location are shown responding to the presence of the device 24 h after implantation. (e) Microglia filopodia investigating the device's surface and neighboring tissue are further presented in this image overlay. Scale bars indicate 200 μm in (a) and (b), and 50 μm in (c–e).